BACHELOR THESIS

Viktor Burian

Study of Lead Tungstate Crystal Scintillators for High Energy Physics Experiments

Department of Low-Temperature Physics

I declare that I carried out this bachelor thesis independently, and only with the cited sources, literature and other professional sources.

I understand that my work relates to the rights and obligations under the Act No. 121/2000 Sb., the Copyright Act, as amended, in particular the fact that the Charles University has the right to conclude a license agreement on the use of this work as a school work pursuant to Section 60 subsection 1 of the Copyright Act.

In Prague, 20 July 2017   Signature of the author:

Title: Study of Lead Tungstate Crystal Scintillators for High Energy Physics Experiments

Author: Viktor Burian

Department: Department of Low-Temperature Physics

Supervisor: Michael Finger,M.Sc.,CSc., Department of Low-Temperature Physics

Abstract: This thesis describes the measurement of the crystal samples of lead tungstate scintillators. New detectors in high energy physics will need high-quality electromagnetic calorimeters. Crytur company in collaboration with researchers from Faculty of Mathematics and Physics develop a method to test optical properties of crystals exposed to radiation. More than one hundred samples were already irradiated and measured to render valuable results. Issues with a spectrometer time stability were revealed and addressed. The significance of temperature influence on radiation induced absorption coefficient is still not fully resolved and is open to further investigation. Correlation between data from Prague and Germany shows that sample measurement is an adequate method to decide crystal quality.

Keywords: FAIR centre, PANDA detector, PbWO crystal, Scintillator, Crytur, Microtron, Radiation induced absorption coefficient

Contents

Introduction

The limits of knowledge in nuclear physics are pushed by more and more sophisticated and complicated devices. The FAIR accelerator facility in Germany will soon be one of these devices.

The PANDA detector is a smaller cousin of CMS and ATLAS detectors at CERN. With new experiments come unresolved challenges. The electromagnetic calorimeter will need scintillator crystals with unprecedented quality.

Half of the crystals were already delivered by the Bogoroditsk Technical Chemical Plant. However after the plant was shut down, the search for a new contractor begun. Intensive research in the field of inorganic scintillators is conducted in research centres around the world. The way to find a receipt to the mass manufacturing process is by gradually refining every step of production. The Czech company Crytur has a long-time experience in crystal fabrication and technology equipment to handle this task.

Growing a crystal is a very expensive process. Additional costs in time and effort are for the cutting and polishing. To save this job in the case of a flawed crystal by measuring its properties a new analytical method is tested.

The goal of this work is to prepare repeatable method of testing small crystal samples in the microtron laboratory to produce good quality measurement results for Crytur. The successful implementation of this method will be validated when the results from the University of Giessen in Germany will correlate with the results from Prague.

At the beginning of the thesis, basic information about the prepared FAIR research centre is presented followed by a more detailed description of the PANDA detector. The second chapter contains overview about electromagnetic calorimeter system. The third chapter addresses principals of scintillation effect and lead tungstate crystal production and operation inside the calorimeter. Chapter four describes the microtron accelerator where the samples are irradiated. It also concisely introduces the principle of gamma radiation production. The fifth chapter presents the results of more than six months of measurement. It starts with the early measurements that verified the methods introduced by researchers from Giessen. Continues with the repeatability measurements and in the end, discusses the results.

1. FAIR - PANDA

1.1 FAIR

The Facility for Antiproton and Ion Research (FAIR) is a research centre currently being built in the area of the GSI in Darmstadt, Germany.

[1] The project collaboration began in 1999. In the year 2006, the FAIR Baseline Technical Report was issued. It described the details of construction of accelerators and experimental setups. The FAIR Green Paper from September 2009 constitutes the plans for the building of the SIS100 synchrotron as the core accelerator and four experiments: APPA (Atomic, Plasma and Applied Physics), NUSTAR (Nuclear Structure, Astro Physics and Reactions), PANDA (AntiProton Annihilation at Darmstadt) and CBM (Compressed Baryonic Matter). In 2010 the international partners founded the FAIR GmbH.

The science objective of the FAIR is to study properties and behaviour of hadronic matter, principals of the strong force and behaviour of the electromagnetic force under extreme conditions. Those objectives can be summarised into finding an answer to these questions:

- Why do quarks never exist in isolation?

- Why are protons and neutrons so much heavier than their constituents?

- In what ratios of protons to neutrons can nuclei exist? What new properties do highly unstable nuclei reveal?

- What fundamental symmetries govern the laws of nature? When, and with what consequences, do violations of such symmetries occur?

Figure 1.1: Artist aerial view on the finished FAIR centre [1]

The accelerator facility begins with linear proton accelerator p-LINAC. The heart of the installation is double-ring heavy ion synchrotron SIS-100. It will deliver high intensity and high energy heavy ion beams to the system of cooling

rings and experiments. The double-ring design will allow operating up to four different experiments simultaneously. The beam energy will be high enough to produce hadrons with charm quark as well as intense antiproton beam. For the plasma research, short ion pulses with a power of several thousand billion watts will be generated.

The properties of the strong force will be studied with proton-antiproton reactions. Scientists believe that new particle called charmonium that consists of one c-quark and one c-antiquark will be produced in such reactions. Examination of this unstable particle should provide insights into the behaviour of the strong force and the confinement phenomenon. The FAIR complex will also help to elucidate the origin of the nucleons masses and possibly discover new states of hadronic matter predicted by the theory of the strong force.
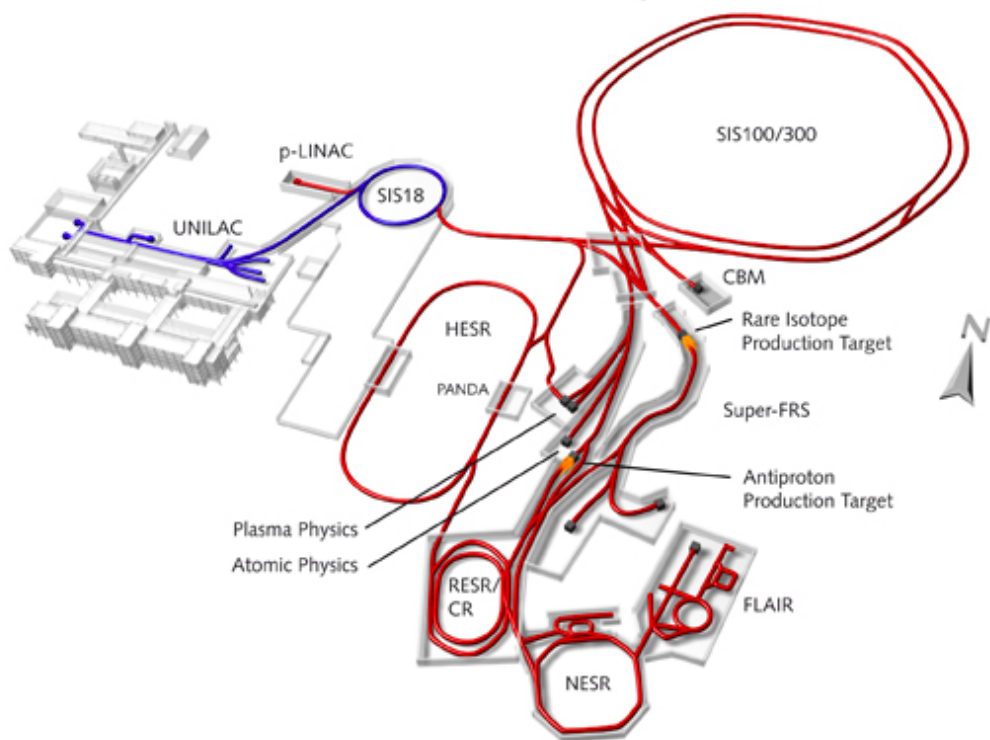

Figure 1.2: Scheme of FAIR accelerators and experiments [1]

1.2 PANDA

The Antiproton Annihilation at Darmstadt (PANDA) experiment is one of the key experiment of the FAIR facility. Antiproton beam from High Energy Storage Ring (HESR) will collide with the fixed target inside the detector. The topics investigated by PANDA will be various. For example hadron spectroscopy, hadrons in nuclear matter, nucleon structure or hypernuclei.

The PANDA Collaboration is 450 scientists from 17 countries. Researchers from Faculty of Mathematics and Physics of Charles University participate on the PANDA project. The Czech contribution to the detector is to manufacture scintillation crystals for the electromagnetic calorimeter.

Inside the detector, millions of proton-antiproton annihilations will take place every second producing plenty of gluons. It is probable that particles called glueballs will be created. Glueballs are short-lived particles made solely from gluons. To study the properties of the Strong force the PANDA detector will search for the glueballs decay. Such event is very rare so the requirements for the detector system are enormous.

The detector itself consists of several components to track the particles' trajectories, measure their energy and to identify the particles' type. The complete detector assembly is in the figure 1.3.
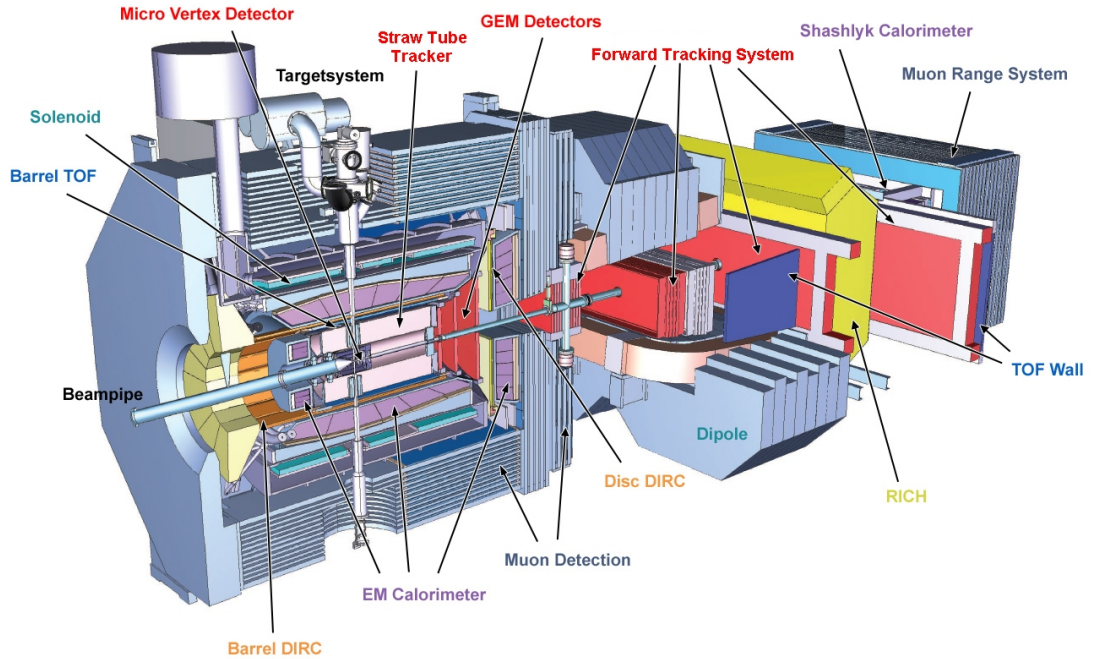

Figure 1.3: Layout of the PANDA detector system [2]

1.2.1 Tracking

The innermost part is the Micro Vertex Detector (MVD). It is the tracking system consisting of silicon pixel and strip detectors. The role of the MVD is to track charged particles with accuracy about $100 \, \mu m$.

Around the MVD is the Straw Tube Tracker. Approximately 30 cm thick cylinder around the beam-target area. It is a set of multiple 150 cm long channel drift tubes filled with a mixture of Argon and CO_2 gasses.

In the forward region, planar Gas Electron Multiplier (GEM) detectors enclose the tracker system. These disks cover polar angles from 3° to 20°. The particle trajectory resolution is better than $100 \, \mu m$.

The last element of the tracking system is the Forward Tracker (FT). The FT is three pairs of planar modules of straw tubes. The first pair is placed behind the GEM detectors. The second pair is placed inside the dipole magnet yoke, and the last pair is behind the dipole magnet. The FT is designed for the momentum analysis of charged particles.

1.2.2 Electromagnetic Calorimeter (ECAL)

The requirements for the ECAL need fast scintillator with a small radiation length. The $PbWO_4$ crystals are used. This material was already used in ECAL in CMS experiment at CERN. The crystal dimensions are $2 \times 2 \times 20 cm^3$. The crystal length is, therefore, $20X_0$.[1] Energy resolution for photons and electrons is thus high. The scintillation light readout will be done by large area avalanche photodiodes for most of the crystals. Only the inner part of the forward endcap will be readout by vacuum phototriodes. The total number of crystals needed for PANDA ECAL is about 16,000. The ECAL will cover almost whole space angle. The crystals are wrapped in highly reflective foil to ensure the total reflection from the crystal edges. Figure 1.4 shows model of the ECAL barrel and forward endcap.
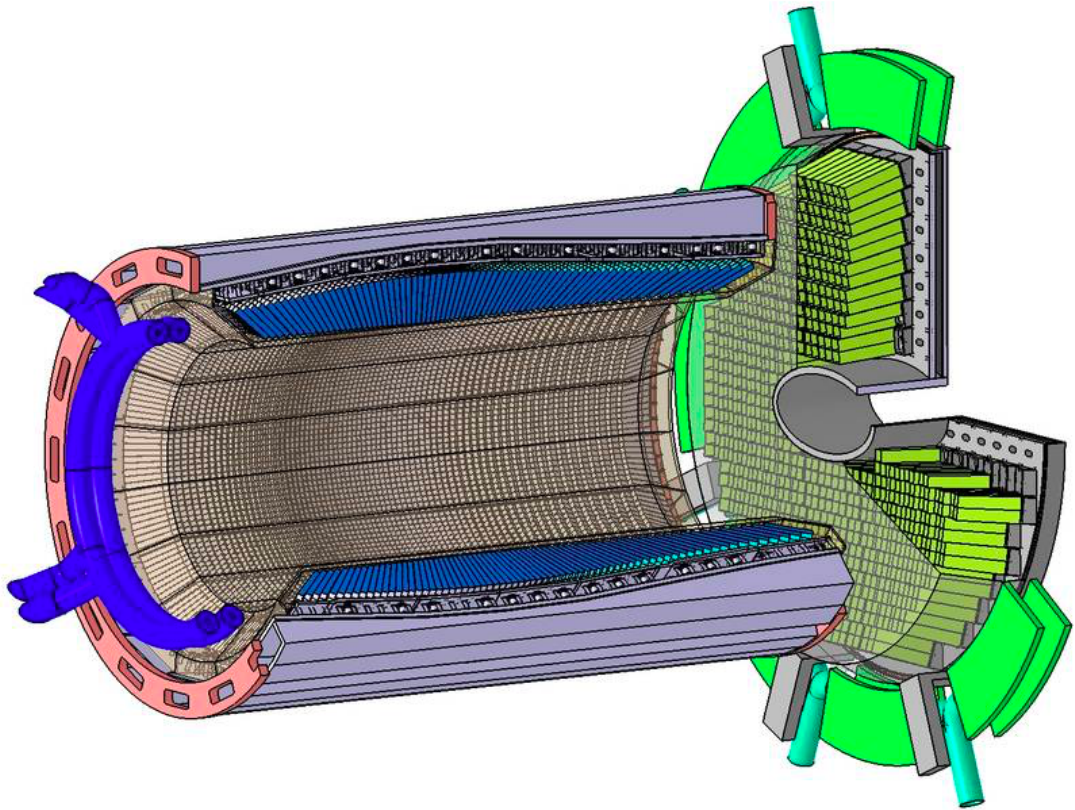

Figure 1.4: Detail of the PANDA ECAL, barrel and forward endcap. The dark blue pipes on the left are the cooling system that will keep the crystals at $-25\,°C$ [2]

1.2.3 Beam Target

Targets in PANDA experiment are designed to be in the form of target beam. Three types are planned.

---

[1]X_0 is the radiation length, a material constant. Mean path over which high energy electron loses all but $1/e$ of its energy by bremsstrahlung.

Cluster target system Cooled beam of hydrogen atoms exhausts from Laval-type nozzles. The expansion of the gas further cools down the atoms and condensation takes place and thus atoms form clusters of about $10^3 - 10^5$ particles.

Pellet target system A beam of frozen hydrogen microspheres flows vertically across the solenoid into the collision area. The speed of the pellets is approx. 60 m/s and a flow rate of 10,000 pellets per second. The pellet undergoes about 100 interactions per second with the antiproton beam. Other gasses like deuterium or noble gasses are also considered.

Nuclear targets A fibre of target material is used instead of clusters or pellets.

1.2.4   Particle Identification

High accuracy in charged particle identification is expected at PANDA experiment. Four different systems are dedicated for the particle ID.

Mass determination The mass of the particles is detected by internally reflected Cherenkov light.

Time of flight system (TOF) For low energy particles and track deconvolution two options are proposed. A fast scintillator or a barrel of Resistive plate chamber counters.

Muon detection system The need for wide muon momentum range identification poses high demands on the identification system. The range system is used as a muon detector. It consists of an iron absorber, target spectrometer, dipole magnet and electromagnetic calorimeter.

Aerogel Ring Imaging Cherenkov Counter (RICH) The aerogel counter with refractive index $n = 1.02$ are designed to provide particle identification and information for a trigger.

1.2.5   Forward Spectrometer

High precision tracking and identification of charged and neutral particles take place in the forward spectrometer which consists of several systems. Some of them are placed inside yoke of the dipole magnet.

1.2.6   Magnet system

The appropriate magnetic field for momentum reconstruction will be produced by two magnets. Solenoid field of strength of $2\,\mathrm{T}$ around the target region and $1\,\mathrm{T}$ strong dipole field in the forward region. Both magnet system with weights of hundreds of tons will be placed on a movable platform for easy commissioning and maintenance.

Solenoid field is provided by superconducting wires cooled by cryostat. The solenoid is $4\,\mathrm{m}$ long and has $1.9\,\mathrm{m}$ in diameter. High level of field homogeneity and number of detector systems placed inside the yoke place high demands on the magnet design.

Dipole magnet will provide the magnetic field for momentum measurement and tracking of particles emitted in the forward spectrometer.

2. PANDA Electromagnetic Calorimeter

2.1 Calorimeter description

Electromagnetic calorimeter (ECAL) measures the energy of particles interacting mainly via electromagnetic interaction. The kinetic energy of incoming particles is transformed into quanta of visible light inside the active volume of ECAL. These quanta are measured by photodetectors. Data collected from photodetectors are processed to give information about the total energy of traversing particles.

PANDA ECAL has three parts. The central barrel which consists of more than 11,000 crystals, forward and backward endcaps. The whole calorimeter covers almost the full space angle. The front face of the barrel crystals will be installed at a 57 cm radius from the beam axis.

Operating temperature of the crystals is $-25\,°C$ to maximise the light yield (LY). The cooling system has to extract the heat created by the read-out electronics and keep the crystals cool within the range of $\pm 0.05\,°C$.

2.2 Photodetectors

Two types of photodetectors will collect the light emitted by the crystals. Avalanche photodiodes (APT) in the barrel region and Vacuum phototriodes (VPT) in the forward and backward endcaps. The vacuum tubes are used because of the high radiation at the forward regions which would damage the photodiodes.

Photodetectors of ECAL must function well in the condition of radiation and magnetic field. Moreover, the APD gain is sensitive to applied bias voltage and working temperature. The VPT gain is much less dependent on high voltage, so it does not need to be controlled that precisely

The energy resolution of the ECAL is a function of the incident energy E in GeV

$$\left(\frac{\sigma}{E}\right)^2 = \left(\frac{a}{\sqrt{E}}\right)^2 + \left(\frac{b}{E}\right)^2 + c^2 \tag{2.1}$$

where a is the stochastic term dependent on an event to event fluctuations and gain, b is the noise term, and c is the constant dependent on the energy leakage from crystal, temperature stability, and detector calibration. Desired value for PANDA ECAL is $\frac{<2\%}{\sqrt{(E)}} + \leq 1\%$. [5]

2.3 Transparency loss

Intense radiation from particle collisions cause defects that decrease the transparency for the crystals.

The transparency changes are needed to observe during the detector operation.

Crystal transparency monitoring is performed using lasers. Two different lasers are used, blue (440 nm) that is close to the emission peak of the lead

tungstate crystal and near infrared (796 nm) that is not affected by the irradiation. The infrared laser is to monitor other changes in detector calibration for example gain of the photo elements. The laser emits pulses with a full width at half maximum ≈ 30 ns with a repetition rate of 80 Hz. For the diagram of laser monitoring system see fig 2.1.
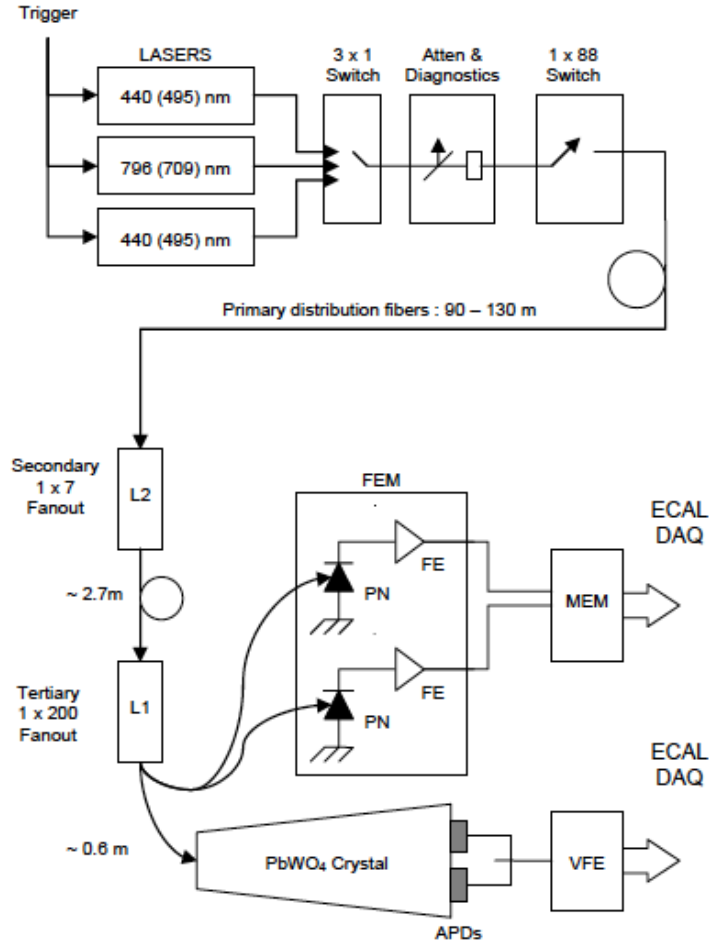

Figure 2.1: Laser monitoring system

The response of crystal photodetector to the laser is compared with the response of PN diode measuring the intensity of light that does not pass through the crystal. Since the scintillation spectrum is different from testing laser light spectrum photodetector responses are also different.

The $R(t) = APD(t)/PN(t)$ is a measure of crystal transparency to laser light at the time t. For changes in transparency less than 10% the relationship between laser and scintillation transparency can be expressed by

$$\frac{S(t)}{S(t_0)} = \left(\frac{R(t)}{R(t_0)}\right)^{\alpha} \tag{2.2}$$

where S is the response to scintillation light and α is the crystal characteristic.

2.4   Preshower detector

The crystal cross-section as stated above is roughly $5\,\mathrm{cm}^2$. Area this big gives rise to a space specification uncertainty. Events, where two closely spaced interacting particles deposit their energy in a crystal, are easy to be mistaken with another event where just one high energy particle stops in a crystal. To reduce such errors, a preshower detector is installed in front of the ECAL. The preshower detector consists of layers of lead and silicon detectors. The silicon detector has much higher granularity than ECAL so It can differentiate single high energy particle from a closely travelling pair. Energy deposited in the preshower detector is measured and added to the energy deposited in the ECAL eventually.

3. PbWO$_4$ crystals

3.1 Scintillator properties

[3] The requirements for PANDA ECAL were to have fast, compact and efficient scintillator. High demands for light yield and radiation hardness determined lead tungstate crystal as a suitable material.

Another important property of the PbWO scintillator is the capability to react to particles in a wide range of energies from MeV to GeV. The speed of scintillation is also significant. About 80 % of the light is emitted within 25 ns.

[4] The main task of the research in the manufacturer is to increase the light yield. Crystals produced for high energy physics for the CMS experiment at LHC did not have to satisfy such high requirements because of the high energy collisions.

Parameter	Value
Density [g/cm^3]	8.23
Moliere radius [cm]	2.2
Radiation length [cm]	0.89
Refractive index at 420 nm [-]	2.24
Light yield at room temperature [photons/MeV]	1-3$\times$10^2
dLY/dT at room temperature [%/°C]	-2.7

Table 3.1: PbWO crystal details [5], [6]

3.2 Scintillation

The scintillation process is based on electron transition between energy bands of the crystal lattice. First, the incoming particle, photon or electron excites atoms of the crystal. Electrons from valence band are kicked to conduction band where they have enough energy to move freely along the lattice. As a result, holes are created in the valence band. Recombination of electrons and holes back to ground state results in photon emission.

To increase light yield and to move emission peak to the region of visible light the crystal is doped with other elements called activators. These impurities form energy levels inside the crystal band gap. Electrons from conduction band then recombine with holes through these states. Energy structure of impurities, as well as the doping, determine the emission spectrum of the scintillator.

The lead tungstate crystals emit blue-green light with a broad maximum at 420 − 430 nm.

3.3 Radiation effects

[7] Crystals are exposed to radiation doses during the detector operation which

influences the transmittance. This effect can be studied on crystal samples irradiated by gamma rays in the accelerator laboratory or by a gamma source.

The quantity that describes the changes in transmittance is the radiation induced coefficient dk. It can be calculated from measured transmittance before and after irradiation:

$$dk\left(\lambda, t\right) = \frac{1}{L} ln\left\{\frac{I\left(\lambda, 0\right)}{I\left(\lambda, t\right)}\right\}, \qquad (3.1)$$

where $I\left(\lambda, 0\right)$ is the transmittance before irradiation, and $I\left(\lambda, t\right)$ is the transmittance after irradiation. The calculated dk includes many other influences from temperature variations, light exposures, spectrometer accuracy, the way the sample was handled and so on.

The process of decreasing transmittance is due to the creation of colour centres by ionising radiation in place of oxygen vacancies. The transmittance decrease is wavelength dependent.

The change of the crystal lattice is reversible. The loss of transmittance is offset by recovery process that is in motion continuously. These two processes act against each other and tend to an equilibrium state. At temperatures around 200 °C crystals are completely annealed, and the vacancies are filled back with the oxygen.

3.4   Crystal production

[3] The raw material the crystals are made of is in the form of powder. Before melting in the furnace, the powder is thermally preprocessed and thickened. The growth takes several days at 1200 °C. Crystals are produced using Czochralski method in the electrically heated furnaces.

Figure 3.1: Precrystal ingot of PbWO

The finished precrystal weights about 2.5 kg. The crystal has a very uneven shape (see figure 3.1). Stress and vacancies inside the crystal are removed by annealing. The final shape is cut by a wire saw machine. The scraps of the lead tungstate material are melted again to produce a new crystal. The finished crystal has rectangular shape 20 cm long, $2 \times 2 \text{cm}^2$ face area and is 1 kg heavy. Cut crystal is then polished to final smoothness.

Transmittance and light yield are tested in the factory before the crystal is sent to irradiation tests to Germany. As a radiation source ^{137}Cs is used with gamma peak at 667 keV.

4. Microtron

4.1 Basic information

[8], [9] The microtron laboratory is part of the Nuclear Physics Institute of the Czech Academy of Sciences. The laboratory is located in the former bomb shelter from the world war two under the Vítkov hill in Prague. Entrance to the underground facility is from the Karlín tunnel.

The first microtron started operation in 1980. Ten years later it was replaced with the newer model MT 25.

The accelerator is situated at the end of a long corridor inside a vault shielded by two heavy doors (see fig. 4.1). Massive rock around the laboratory reduces the cost of gamma radiation shielding.

The microtron can deliver electrons with the maximum energy of 25 MeV. Maximal mean electron current is 25 μA [10]. Secondary gamma radiation is produced in a radiator plate by bremsstrahlung. Even tertiary neutron radiation produced in photo nuclear reactions can be used at microtron.
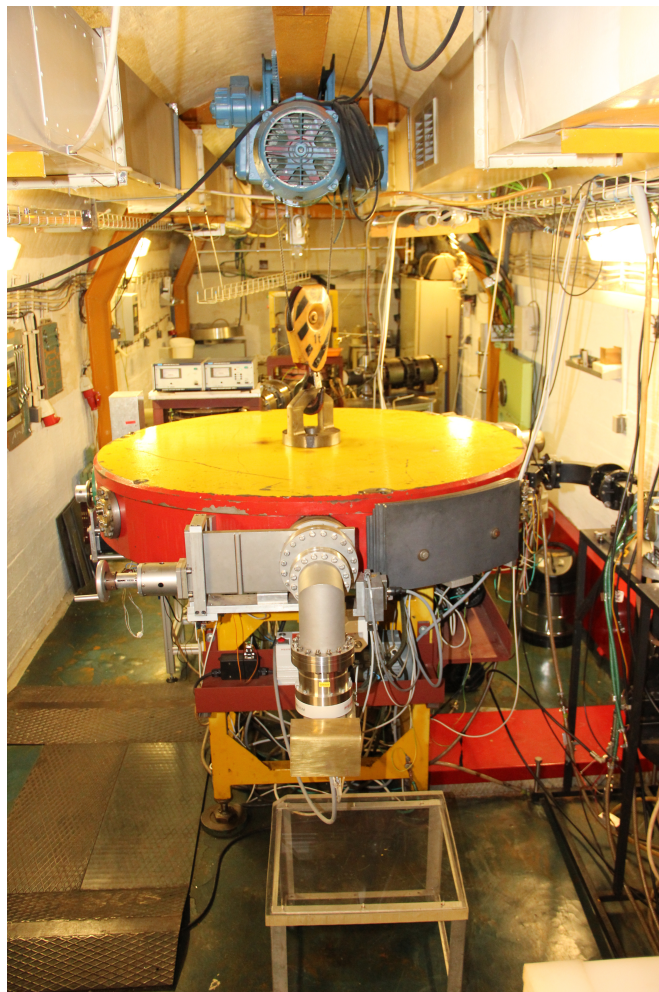
Figure 4.1: Microtron vault with the vacuum chamber in the foreground

4.2   Princip of acceleration

Microtron is a cyclic electron accelerator. Electrons orbit circular trajectories with a common tangent point. This point is at the resonant cavity. With every revolution, an electron gets an integer multiple of its rest energy. Moreover, the period of revolution will also be the integer multiple of the original period. So the electron arrives at the resonant cavity at the time when the phase of the accelerating radio frequency field is same as at the last arrival. Electron gets another boost and travels on higher orbit. Extracted electron beam is highly monoenergetic.

4.3   Parts of the microtron

Magnetron The magnetron oscillator is the source of radio frequency (RF) waves with frequency of $2.9\,\mathrm{GHz}$ with a constant amplitude.

Acceleration resonant cavities A stable acceleration is provided by coincident frequencies of oscillator and resonant cavity. Frequency control system with a coupler is incorporated to keep the frequencies within appropriate limits.

Magnet Hollow copper leads of the electromagnetic coil inside the vacuum chamber generate a constant uniform magnetic field (see fig. 4.2). The hollow leads enable inner water cooling.

Figure 4.2: View inside the vacuum chamber

Electron extraction at variable energies Telescopic tubes controlled remotely from control room enables to select electron orbit and extract electrons from the accelerator (see fig. 4.4). Electron beam is guided to one of the three output terminal (see fig. 4.5). Automatic beam position stabilisation control and current measurement are in two of the three exit channels. Titanium $0.05\,\mathrm{mm}$ thin foil separates vacuum system from the workspace.

Control room Next to the shielding doors outside the vault is the control room (see fig. 4.6). From here accelerator parameters and setting are regulated

and checked. The control system is automated so it can run the accelerator without human intervention. An operator is required to check the key parameters of the system and in case of anomaly turn of the accelerator. From here the carousel motor is switched.
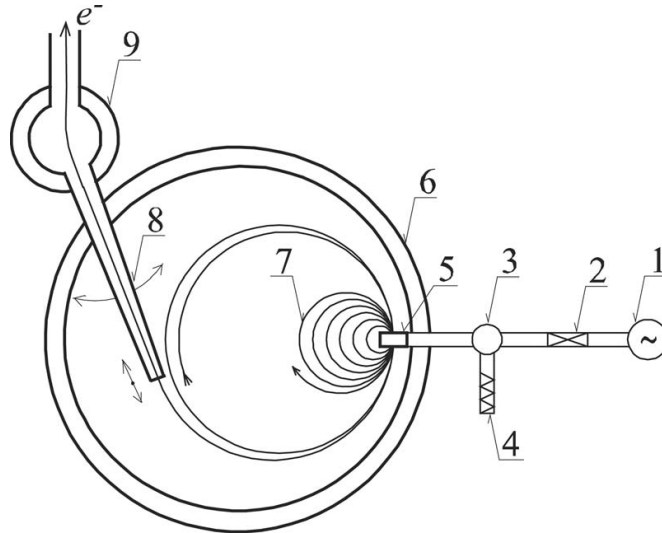

Figure 4.3: Schematic layout of the microtron MT25. 1: magnetron, 2: phase shifter, 3: circulator, 4: water load, 5: accelerating cavity, 6: main magnet (vacuum chamber), 7: electron trajectories, 8: adjustable beam extractor, 9: first deflector [10]

4.4 Gamma ray production

[11] Gamma rays are produced by bremsstrahlung in tungstate strip called converter mounted at the end of output nozzle. For energy 5.5 MeV the width of the converter is 2 mm, for 16.6 MeV the width is 2.5 mm, and the additional aluminium cylinder is placed after the converter to capture all electrons coming through the tungstate strip (see fig. 4.7).

The gamma beam has a diameter of 5 cm and power density homogeneity better than $\pm 5\%$. The gamma rays have a continuous spectrum with an edge at the electron energy.

Figure 4.4: Adjustable iron channel for electron extraction
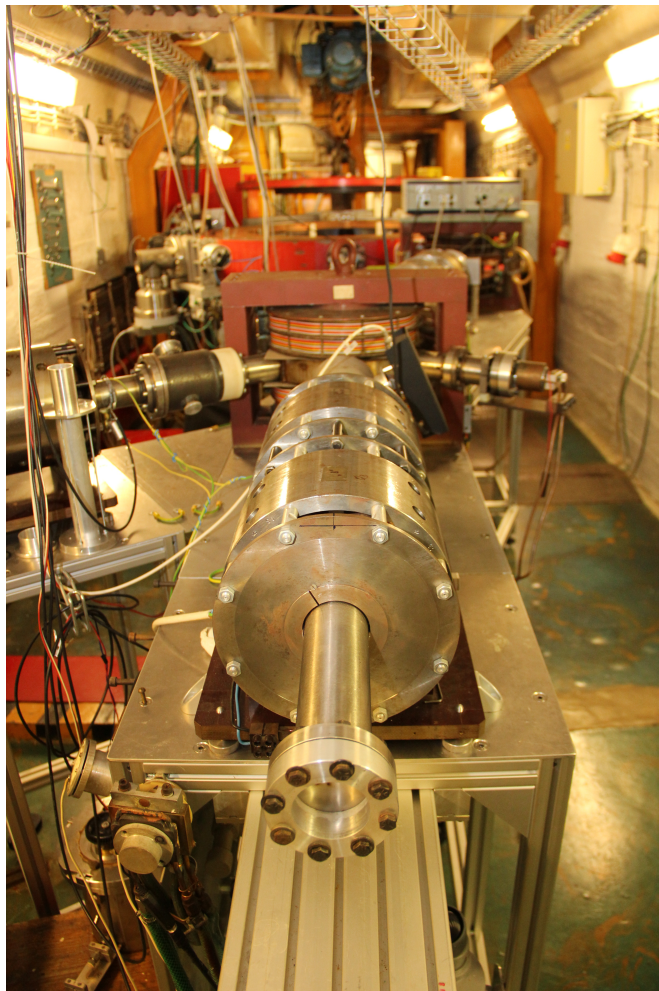
Figure 4.5: Output nozzles at workspaces

Figure 4.6: Microtron control panel
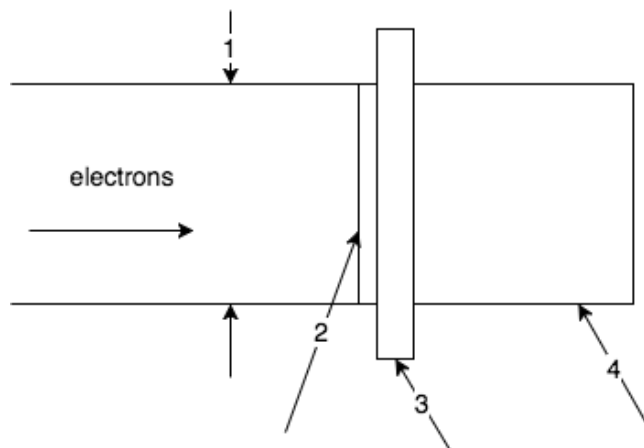
Figure 4.7: Output nozzle schematic. 1: 50 mm diameter electron beam line, 2: Titanium foil, 3: Tungstate converter, 4: Aluminium cylinder

5. Measurement

5.1 Measurement procedure overview

Measurement of the radiation induced absorption coefficient is a set of several steps. Before a measurement can be conducted, samples must be annealed to eliminate crystal defects. The first step is to measure the transmittance of the sample in a spectrometer. The second step is to irradiate the sample by gamma rays. The last step is to measure the transmittance again after a specified period. To guarantee repeatability it is necessary to obey the measurement procedure. Every incorrectly performed operation is a source of errors. Following are the steps written in details to make the impression what the process involves.

- Annealing samples before measurement in a furnace for at least 200 °C for 2 hours.

- Samples must be placed in a Petri dish covered with a lid to prevent organic substances react with sample's surface.

- The spectrometer lamp has to be turned on at least half an hour before the measurement.

- Sample compartment in spectrometer must be empty and clean.

- Every sample is transported inside a tissue that has the identification number written on it. So has the sample. Both ID numbers must match.

- Samples' sides are usually cut with only one right angle. These sides are marked with dots and ensure not ambiguous position inside the sample compartment.

- The thickness of a sample is measured with a digital caliper (resolution $< 0.1\,\mathrm{mm}$).

- If a sample is dirty, the surface is cleaned with ethanol. Otherwise only a short blow of compressed air from spray is sufficient to remove dust.

- Standard Correction on spectrometer is run before every transmittance measurement

- Sample transmittance is measured before irradiation

- The carousel position and height is located to the beam axis by laser meter.

- Carousel rotation is turned on during the whole measurement

- The sample is placed on the carousel, see figure 5.1.

- Doors of the microtron vault are closed, and the sample is irradiated.

- The irradiated sample is put inside a box to prevent unintended light exposure.

- After 30 minutes the irradiated sample is measured in the spectrometer.

Generally, for two conditions must be paid attention. Light and temperature. Both can affect the crystal defects inside the samples and devalue the measurement. Therefore only a dim light in the spectrometer room can be turned on and no light at all in the microtron vault.

There should be thirty minutes period when the sample is in a dark place at a constant temperature. Processes inside the crystal right after the irradiation are under way, and immediate transmittance measurement would be affected by the systematic error.

The distance between the gamma source and a sample is approximately half a meter as seen in the figure 5.2. The dose absorbed inside the crystal decreases with the depth. Rotation of the sample during irradiation helps to increase the homogeneity of the absorbed dose.

The radiation hardness also depends on the doping with other elements. Dopant concentration varies while the crystal grows. Thus to have additional information about how doping influences the optical properties two sample blocks are cut from the ingot. Each sample size is $2 \times 2 \times 1 \text{cm}^3$.
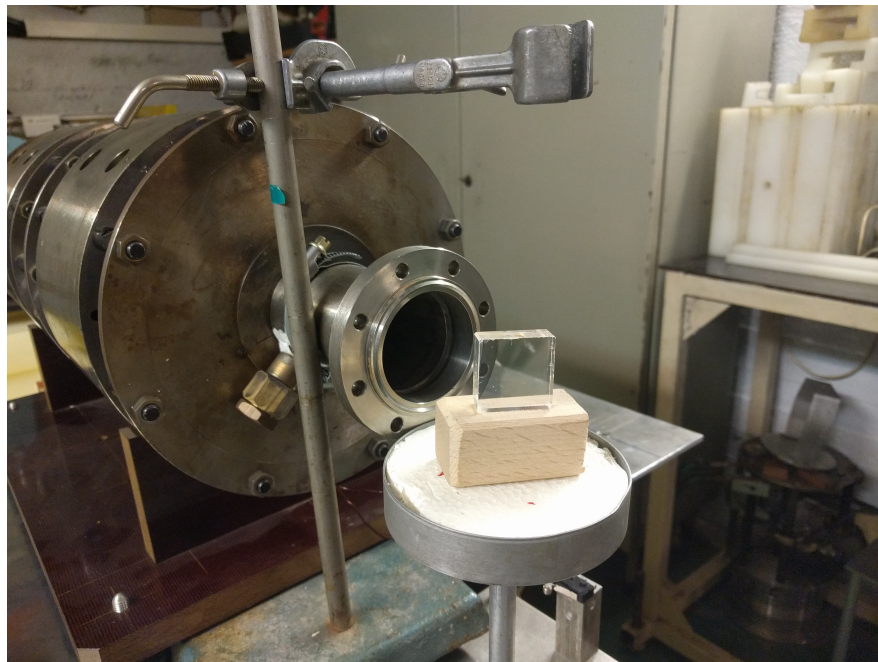
Figure 5.1: Sample crystal on the carousel

5.2 Irradiation settings

The first measurement in Prague was done in October 2016. Since then more than one hundred samples were measured.

There was a discussion what energies of electrons to set on microtron. At the beginning 10 MeV electron beam was used for ten samples. However, the energy of the electron beam can be changed only when the accelerator is open and such operation is arduous. Most common energy used is 16.6 MeV. To decide if the

Figure 5.2: Sample crystal and the microtron nozzle

change to higher energies is possible a control measurement was performed on reference samples. Radiation induced absorption coefficient for the whole set of reference samples is shown in figure 5.3 for both electron energies. There are differences between the curves however it was decided that the change to higher energies is possible.

Another irradiation variable is the dose rate. First samples were irradiated with the dose rate around $0.01\,\mathrm{Gy/s}$. Total irradiation time was 900 seconds and the total dose was $10\,\mathrm{Gy}$. Higher dose rates were studied to reduce the time needed for one sample. $600\,\mathrm{s}$, $400\,\mathrm{s}$, $200\,\mathrm{s}$ and $100\,\mathrm{s}$ irradiation intervals were tested with the same total dose received by the samples. Results of this tests for the reference samples are in the figures 5.4, 5.5, 5.6 and 5.7. 200 seconds was chosen as an optimal irradiation period which is $0.05\,\mathrm{Gy/s}$ dose rate.

Absorption at the long wavelength is not affected by the radiation. Radiation induced coefficient should be zero at around $800\,\mathrm{nm}$ and longer wavelength. Non-zero values of dk at near infrared region mean instrument error. All dk curves are offset to zero at $800\,\mathrm{nm}$ for better comparison of results.

5.3 Transmittance measurement

The transmittance measurement is conducted on a laboratory spectrometer. [12] The spectrometer Specord 200 from the company Analytik Jena was delivered from Germany. It can measure the transmittance in the range from $300\,\mathrm{nm}$ to $900\,\mathrm{nm}$ with a resolution of $1\,\mathrm{nm}$ and accuracy less than $\pm0.5\,\mathrm{nm}$. For UV range the light source is deuterium lamp, and for visible range, the light source is a halogen lamp. Light from the light source is monochromatized, split into sample and reference beam and measured by two temperature-controlled diodes. Set of filters, concave grating and slit assembly work as a monochromator. Measure-
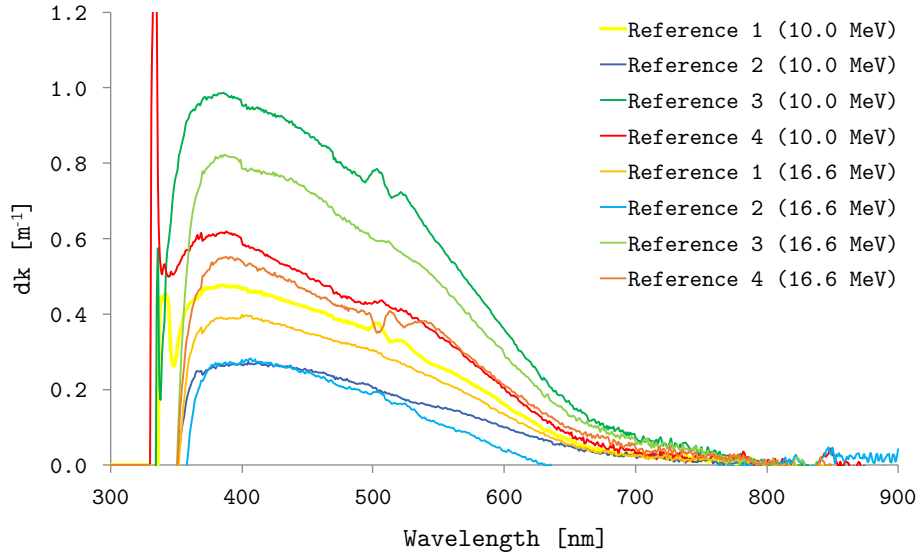
Figure 5.3: Comparison of the radiation induced absorption coefficients for the reference samples at 10.0 MeV and 16.6 MeV

ment is fully automatic and controlled by a program. Stepper motor changes the filter and grating position to select the desired wavelength. The schematic of mechanical components is in figure 5.8.

An example transmittance curve for a sample with ID 161 - measured on 13 July before irradiation is at figure 5.9. Very strong absorption in the region until 330 nm can be observed. That is why dk curves in graphs have this part replace by zeros to suppress pointless very large values of dk. 10 Gy dose change the transmittance of about 0.5 % in the region of the scintillation maximum at 420 nm.

5.4   Repeatability issues

The basic postulate of a good measurement is a repeatability. If a measurement is conducted again with the same conditions, the results should be the same or at least inside a tolerance.

The first results from Prague were significantly different from the results from Germany where the whole crystals are measured using source ^{60}Co. That was an incentive to verify repeatability at microtron laboratory. The transmittance of a sample was measured at spectrometer within a short period without irradiating. The results differed substantially. A spectrometer measurement was identified as a source of big error.

It was decided to perform a standard correction before every transmittance measurement to calibrate the spectrometer. A set of samples was repeatedly
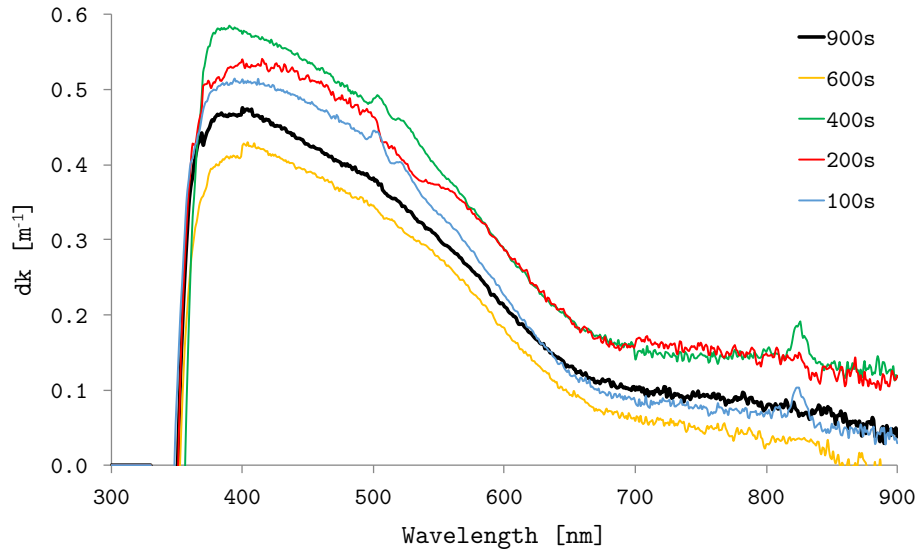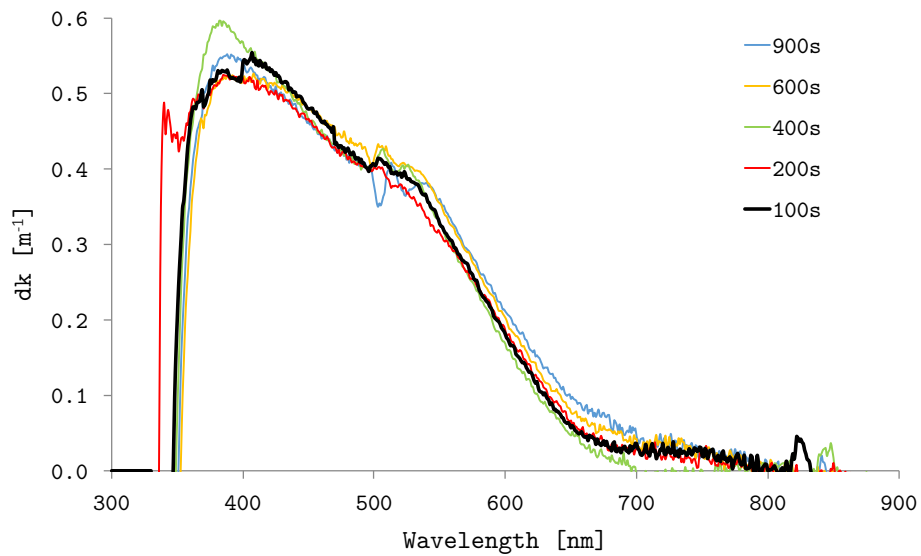
Figure 5.4: Radiation induced absorption coefficient at different irradiation time intervals for the reference sample number 1

measured including irradiation. Before every test, the sample was completely annealed. Results for two of these samples are at figures 5.10 and 5.11. The difference between every measurement was decreased and the data from Prague correlate with the data from Germany.
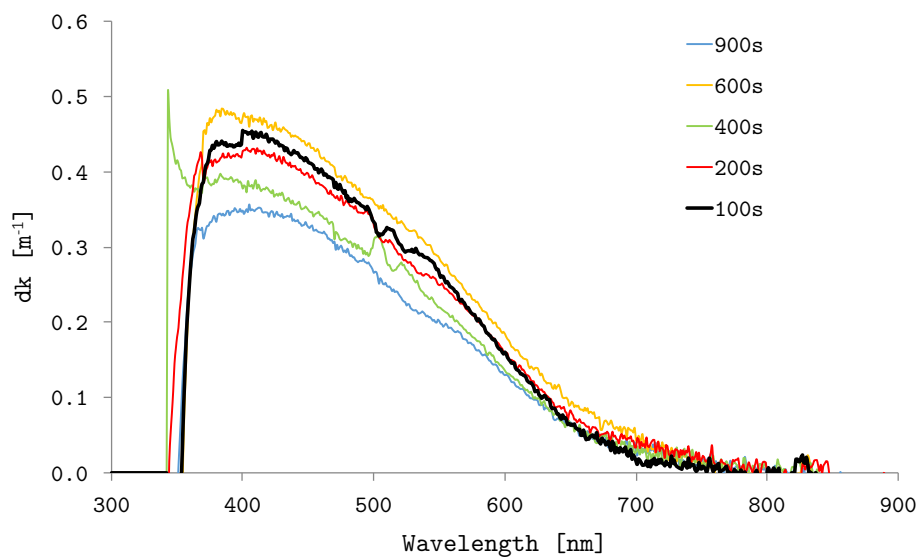
Figure 5.5: Radiation induced absorption coefficient at different irradiation time intervals for the reference sample number 2
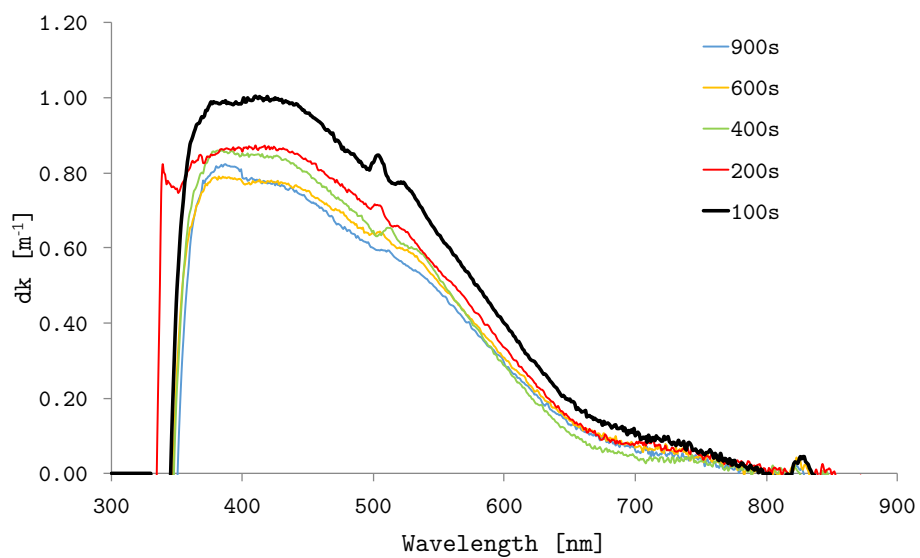
Figure 5.6: Radiation induced absorption coefficient at different irradiation time intervals for the reference sample number 3

Figure 5.7: Radiation induced absorption coefficient at different irradiation time intervals for the reference sample number 4
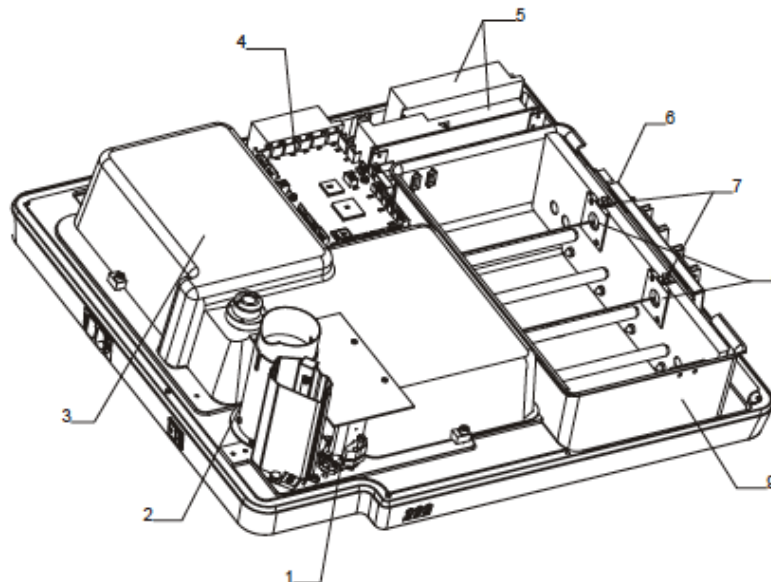
Figure 5.8: Mechanical design of Specord 200 spectrometer. 1: Toric illuminating mirror, 2: Light sources, 3: Cover of spectrometer system and photometer section, 4: Device control, 5: Power supply module, 6: Detector board, 7: Holder for turbid samples, 8: Mount for standard cell holder, 9: Sample compartment [12]
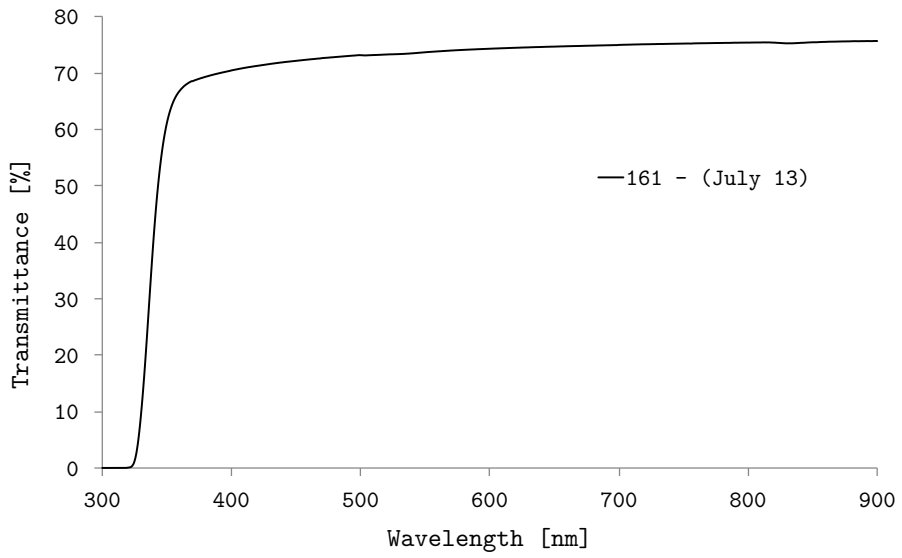
Figure 5.9: Transmittance curve of sample with ID 161 - measured before irradiation
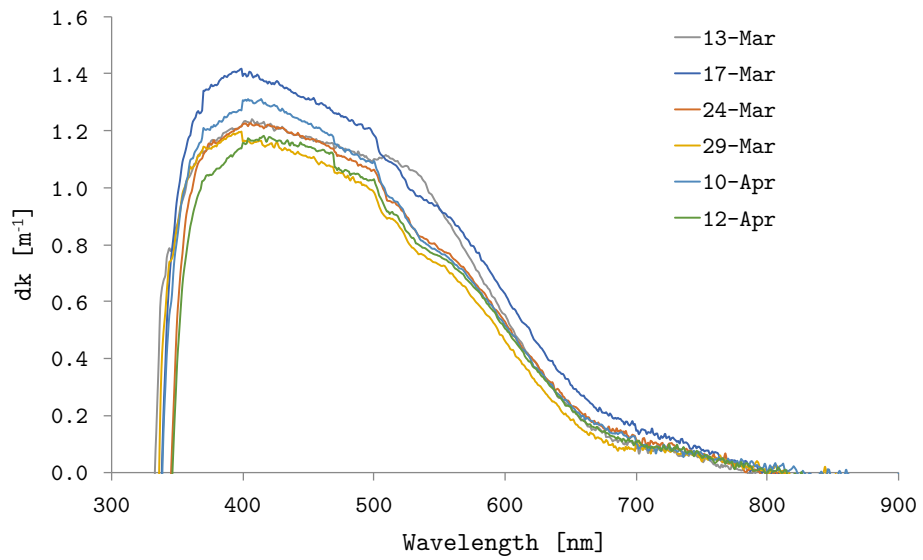
Figure 5.10: Repeatability measurement for sample with ID 135 -
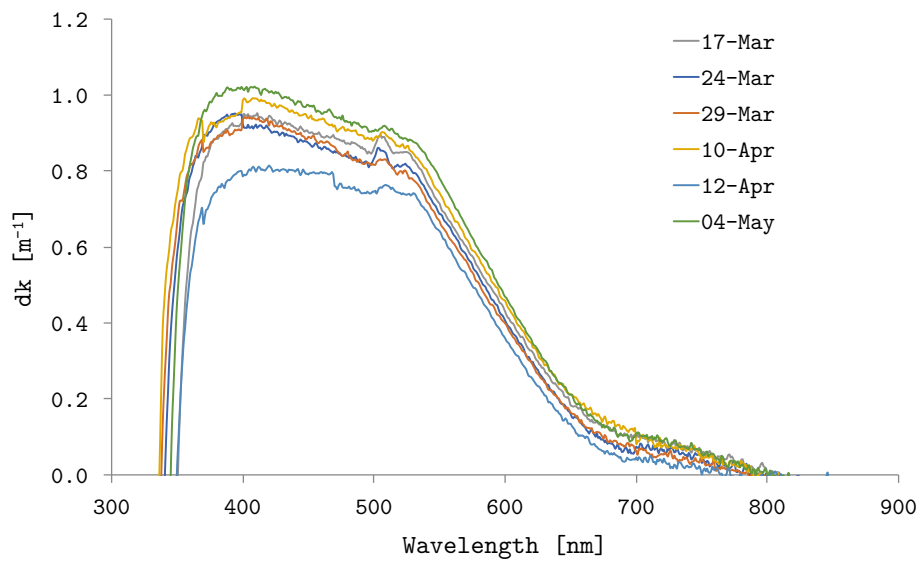
Figure 5.11: Repeatability measurement for sample with ID 141 -

Conclusion

In this work, the plans for the new accelerator and research centre being built at GSI in Darmstadt were introduced. A brief description of the PANDA detector and its components was delivered. The main focus was on the electromagnetic calorimeter and the PbWO4 crystals. The Czech company Crytur tender for delivery of 8,000 scintillator crystals for the PANDA calorimeter. Intensive research is conducted to produce crystals in desired quality.

A method to test crystal sample was developed in collaboration with microtron laboratory. The sources of the biggest inaccuracies and errors were addressed. The extensive knowledge about crystal sample testing was accumulated and will be transferred to other researchers. The issue that still has to be resolved is the relatively big spread of data from sample measurements. The temperature instability during testing apparently causes the variations. The following research in measurement process will be concentrated on minimizing variations between results.

Bibliography

[1] FAIR center home page. `http://www.fair-center.com`, July, 2017.

[2] PANDA experiment home page. `https://panda.gsi.de/oldwww/`, April, 2017.

[3] Rainer W. NOVOTNY, Valera DORMENEV, Mikhail KORJIK, Jindrich HOUZVICKA, and Hans-Georg ZAUNICK. New Lead Tungstate Crystal Production for High- Energy Physics Experiments Based on the Czochralski Technique. *2015 IEEE Nuclear Science Symposium and Medical Imaging Conference (NSS/MIC)*, 2015.

[4] CMS Colaboration. Performance and operation of the CMS electromagnetic calorimeter. *Journal of Instrumentation*, 2010.

[5] CMS Collaboration. The CMS Experiment at the CERN LHC. *Journal of Instrumentation*, 2008.

[6] PANDA Collaboration. Technical Design Report for: PANDA Electromagnetic Calorimeter. Technical report, Facility for Antiproton and Ion Research, October, 2008.

[7] M. SULC, A. G. BELOV, D. CHVATIL, and et al. The study of PbWO4 crystal scintillators sensitivity to gamma and neutron irradiation. *Czechoslovak Journal of Physics [online]*, 49:183–188, 1999.

[8] M. Vognar, Č. Šimáně, and D. Chvátil. Twenty Years of the Microtron Laboratory Activity at CTU in Prague. *Acta Polytechnica*, 43(2/2003), 2003.

[9] Pavel KRIST and Jiri BILA. A mathematical model of the MT 25 microtron. *Journal of Instrumentation Journal of Instrumentation Journal of Instrumentation*, 2011.

[10] M. Králík, J. Šolc, D. Chvátil, P. Krist, K. Turek, and et al. Microtron mt 25 as a source of neutrons. *Review of Scientific Instruments*, 2012.

[11] M. VOGNAR, Č. ŠIMÁNĚ, A. BURIAN, and D. CHVÁTIL. Electron and photon fields for dosimetric metrology generated by electron beams from a microtron. *Nuclear Instruments and Methods in Physics Research Section A: Accelerators, Spectrometers, Detectors and Associated Equipment [online]*, 380:613–617, 1996.

[12] Analytic Jena AG. *Specord PC 200*, April, 2005.

List of Figures

List of Tables

List of Abbreviations

APPA	Atomic, Plasma and Applied Physics
APT	Avalanche Photodiode
ATLAS	A Toroidal LHC Apparatus
CBM	Compressed Baryonic Matter
CERN	the European Organisation for Nuclear Research
CMS	Compact Muon Solenoid
DIRC	Detection of Internally Reflected Cherenkov Light
ECAL	Electromagnetic Calorimeter
FAIR	Facility for Antiproton and Ion Research
FT	Forward Tracker
GEM	Gas Electron Multiplier
GSI	Gesellschaft für Schwerionenforschung
HESR	High Energy Storage Ring
LHC	Large Hadron Collider
LY	Light yield
MVD	Micro Vertex Detector
NUSTAR	Nuclear Structure, Astro Physics and Reactions
PANDA	Antiproton Annihilation at Darmstadt
p-LINAC	Proton Linear Accelerator
RF	Radio frequency
RICH	Aerogel Ring Imaging Cherenkov Counter
SIS100	Superconducting Synchrotron
TOF	Time of Flight
UV	Ultraviolet
VPT	Vacuum phototriode